

Supporting Information

Generating signals at converging liquid fronts to create line-format readouts of soluble assay products in three-dimensional paper-based devices

Ibrahim H. Abdullah[†], Daniel J. Wilson[†], Andrea C. Mora, Rayleigh W. Parker,
and Charles R. Mace*

Department of Chemistry, Tufts University, Medford, MA 02155

[†] Authors contributed equally.

*Corresponding author email: charles.mace@tufts.edu

Pages: 24 **Figures:** 11 **Tables:** 6

Contents: Materials and Methods. Considerations for device assembly. Tables and graphs describing layer treatment and design that control device and assay performance, methods to analyze signal intensities, schemes for Fe(III), acetylcholinesterase, lactate, and multiplexed assays.

Materials and Methods

Reagents and Device Materials

We purchased Whatman chromatography paper grade 4 (GE Healthcare Life Sciences) from Amazon. We purchased Ahlstrom chromatography paper grade 54 and 55 from Laboratory Sales & Services LLC. We purchased Ahlstrom chromatography paper grade 601 and 613 from Thomas Scientific. We purchased Flexmount Select DF051521 (permanent adhesive double-faced liner) from FLEXcon. We purchased Fellowes laminating sheets and Grass Green food color from Amazon. We purchased Allura Red AC from TCI. We purchased Trypan Blue from Invitrogen. We purchased Iron(III) chloride hexahydrate, 3-(2-pyridyl)-5,6-diphenyl-1,2,4-triazine-*p,p'*-disulfonic acid (Ferrozine), nicotinamide adenine dinucleotide (NAD⁺), and phenazine methosulfate (PMS) from Acros Organics. We purchased ethylenediaminetetraacetic acid disodium salt dihydrate, acetylthiocholine chloride, L-lactate dehydrogenase, Acetylcholinesterase (AChE) from *Electrophorus electricus* (electric eel), 3-(4,5-dimethylthiazol-2-yl)-2,5-diphenyltetrazolium bromide (MTT), glycine, and hydrazine sulfate from Sigma Aldrich. We purchased iron(II) chloride tetrahydrate, L-ascorbic acid, DL-cysteine, 5,5'-dithiobis(2-nitrobenzoic acid) (DTNB, Ellman's reagent), and sodium L-lactate from Alfa Asar. We purchased Tris buffer from VWR. We purchased 10X phosphate buffered saline (PBS) from Fisher Scientific. We purchased ASTM Type I water from Ricca Chemical Company. We used an EPSON Perfection V600 Photo scanner to acquire images of devices and completed assays.

Solution preparation

For the Fe(III) assay, we prepared solutions of Ferrozine, L-ascorbic acid, and EDTA in Type I water. To test the effect of changing the EDTA concentration on the S:B produced by the assay, we prepared different concentrations of EDTA (10–500 mM). To test the effect of changing the Ferrozine concentration on the S:B produced by the assay, we prepared different concentrations of Ferrozine (10–100 mM). For the calibration curve, we prepared different

concentrations of $\text{FeCl}_3 \cdot 6\text{H}_2\text{O}$ (5.6–13 mM). For device layer treatments, we deposited 2 μL of 100 mM EDTA on one side of the sample distribution layer (device layer 2). We then deposited 0.5 μL of Ferrozine (100 mM) on the same side as the EDTA treatment and ascorbic acid (100 mM) on the opposite side of the reagent storage layer (device layer 3). To dry deposited reagents, we incubated the device layers in the oven for 20 minutes at 65 °C.

For the acetylcholinesterase (AChE) assay, we prepared fresh samples of different concentrations of AChE (2–30 U/mL) in 50 mM Tris buffer (pH 8) daily. We prepared 75 mM of acetylthiocholine chloride and 30 mM of Ellman's reagent (DTNB) in 100 mM PBS (pH 7.4). For device layer treatments, we deposited 0.5 μL of acetylthiocholine chloride and DTNB on opposite sides of the reagent storage layer (device layer 3). To dry deposited reagents, we incubated the device layers in the oven for 20 minutes at 65 °C.

For the lactate assay, we prepared a NAD^+ /LDH solution by mixing 45 μL of NAD^+ (30 mM) and 7.5 μL of lactate dehydrogenase (LDH, 1 mg/mL) in 97.5 μL of Type I water. For this mixture, we freshly prepared both NAD^+ and LDH solutions using DI water. We prepared 10 mM solutions of PMS and MTT in Type I water. We prepared glycine-hydrazine buffer by dissolving a mixture of hydrazine sulfate, glycine, and EDTA (disodium dihydrate) in Type I water. The hydrazine buffer was stored in an amber bottle at 4 °C until use. The final buffer concentrations of hydrazine sulfate, glycine, and EDTA were 500 mM, 850 mM, and 15 mM respectively. The final pH of the hydrazine buffer was 9.7. To prepare the device, we deposited 2 μL of the NAD^+ /LDH mixture and 10 mM of MTT on opposite sides of the sample distribution layer (device layer 2). On the reagent storage layer (device layer 3), we deposited 1.5 μL of the NAD^+ /LDH mixture in the corresponding zone to the previous addition on the second layer. On the other side of the reagent storage layer (device layer 3), we deposited 1.5 μL of 10 mM PMS. On the interface formation layer (device layer 4), we deposited 2.5 μL of glycine-hydrazine buffer (pH 9.7) on the side that would be under the NAD^+ /LDH mixture treatments. We dried all treated paper layers in the dark room at room temperature for one hour.

For the multiplexed assays, we prepared all the reagents using the same concentrations and solvents as the singleplex assays. For the positive controls, we prepared a 5 mM solution of $\text{FeCl}_2 \cdot 4\text{H}_2\text{O}$ in Type I water and a 500 mM solution of cysteine in ethanol. The conditions for the treatment of specific device layers for all the assays are shown graphically in **Figure 3** (Fe(III)), **Figure S9** (AChE), **Figure S10** (lactate), and **Figure S11** (multiplexed detection of Fe(III) and AChE with controls).

Iron assays in standard geometries of paper-based devices.

Similar to the conditions used to detect Fe(III) in the devices where readouts are performed at interfaces (e.g., **Figure 3**), we fabricated and treated two alternative device designs where assays are conducted in zones that are more standard to paper-based microfluidics: in single zones and at the end of a channel. Single-layer devices comprise circular zones with a diameter of approximately 5 mm (**Figure S1A**). We treated each zone with 0.5 μL of both 100 mM ascorbic acid and 100 mM Ferrozine. Devices received 1 μL of Fe(III) at different concentrations. Channel-based devices are simple three-dimensional devices that comprise a circular sample inlet before terminating in a channel where readout is performed (**Figure S1B–C**). We treated the sample inlet with 2 μL of 100 mM ascorbic acid, while the end of the channel received 2 μL of 100 mM Ferrozine. Channel length is approximately 10 mm and circular zones have a diameter of approximately 5 mm. Devices received 14 μL of Fe(III) at different concentrations. All layer treatments were dried for 7 minutes at 65 °C prior to assembly and use.

Fabrication of paper devices

We used Adobe Illustrator to design the device layers and then printed the hydrophobic wax barriers using a Xerox ColorQube 8570 wax printer. We cut all adhesive layers using a Boss laser cutter (BOSS-LS1630). We used a Promo Heat CS-15 T-shirt press (45 seconds at 138 °C) to melt the wax onto the chromatography paper to form hydrophobic barriers. Using a custom

acrylic alignment jig (**Figure S3**), we laid the adhesive onto the chromatography paper and compressed both layers together. Next, we sent the chromatography paper attached to the adhesive through a laminator (Trulam) to remove any air bubbles trapped between the layers. The device layers were then treated with their respective assay reagents. After reagent treatment, we assembled the device layers using the custom acrylic alignment jig. Finally, we cut a strip of a Fellowes laminating sheet, adhered it under the readout layer of the device, then compressed with the laminator once again. The laminating sheet serves as a layer that prevents evaporation of water from the product solution formed.

Device Manufacturing Considerations

In early prototypes of these three-dimensional paper-based microfluidic devices, we observed that the formation of interfaces centered within detection zones can be hindered by misaligned device features or asynchronous arrival of fluid fronts to the test zone. Inconsistencies in the time delay required to form products at interfaces after samples had been added, as well as variability in the position of interfaces across replicate measurements, precluded quantitative analysis of assay results. These first devices were fabricated using a manual layer alignment technique with poor tolerances that did not provide sufficient reproducibility to compare replicate measurements. To ensure that these device layers are consistently aligned, meaning that interface position is only dependent on the synchronized delivery of fluid fronts to the detection zone, we developed the layer alignment pin tool (**Figure S3**). After preparation of adhesive-backed sheets, cut strips of device layers can be assembled on the alignment tool using punched alignment holes at the ends of each strip. Alignment holes patterned in the adhesive sheet by laser cutting can be used as guides for the hollow punch used to form the alignment holes in paper. After a strip of multilayered devices has been assembled on the alignment pins, their layers can be pressed together by hand or with the acrylic top plate before being laminated in a protective slip. This approach consistently provided interfaces at the center of device detection zones when

reagents stored on either side of the device have comparable rehydration requirements and solution flow rates.

Influence of channel and readout zone geometry on the position of formed interfaces.

We studied the impact that the channel length and width and readout zone shape have on the positioning of formed interfaces. We added 1 μL of yellow and blue food coloring on opposite sides of the reagent storage layer of our full, four-layer device. We dried all reagents for 7 minutes at 65 $^{\circ}\text{C}$, then added 30 μL of DI H_2O to initiate flow. We scanned devices after 3 minutes and used Line and Plot Profile tools in ImageJ to measure the positions of formed interfaces within the readout zone (**Figure S4**). If the interface formed off-center to the left, measurements were assigned a negative value, while positive values were assigned to interfaces formed off-center to the right; interfaces perfectly in the center of the readout zone have a measured offset of 0 mm.

We measured the position within the readout zone where interfaces formed using devices that varied in channel width (2, 3, and 4 mm) and channel arm length (7, 10, and 13 mm). These data are compiled in **Table S1**. We observed that channel width had minimal impact on the accuracy of the interface position, with 3-mm channels having modestly better precision than channels that were narrower or wider. Channel length, however, did have a substantial effect on either the accuracy or precision of the interface position, where 10-mm channels had the best performance. Accordingly, we selected 3 x 10 mm channels for all further experiments. We also varied the shape of the readout zone and compared square, circular, and straight zones where interfaces would form (**Table S2**). All three shapes formed interfaces with similar accuracies and precisions, and we selected circular test zones for all further experiments.

Influence of sample volume on the position, width, and intensity of formed interfaces.

We used an Fe(III) assay to investigate the effect of applied sample volume on the absolute position, width, and color intensity of interfaces formed in our paper-based devices. We found that the minimum volume required to rehydrate stored reagents and drive liquid fronts to converge in the readout zone was 14 μL . However, it would be desirable to determine the range of volumes that were suitable for assays to be performed reproducibly and not just at the minimum where any errors in sample application could lead to a device failure. We performed assays with sample volumes between 20–100 μL and measured offset distances of the formed interface, the width of the interface 7 minutes after formation of color, and the intensity of the red channel in the scanned image (**Table S4**). While all volumes above 20 μL had similar offset distances and channel widths, only volumes above 30 μL had reached a plateau in the intensity of the interface signal and no benefit was observed to using larger volumes. We therefore chose to use 30 μL sample volumes to develop all singleplex assays.

Figure S1. Comparison of signal formation for a colorimetric assay for Fe(III) in different paper device geometries treated with Ferrozine and ascorbic acid. (A) Zones patterned in single layers of paper produce a purple reaction product that is difficult to differentiate at different concentrations of Fe(III) and with a non-monotonic increase in intensity. (B) Channels positioned at the ends of simple three-dimensional devices (C) produce non-uniform distributions of color whose intensities and positions make qualitative and quantitative interpretations difficult to perform.

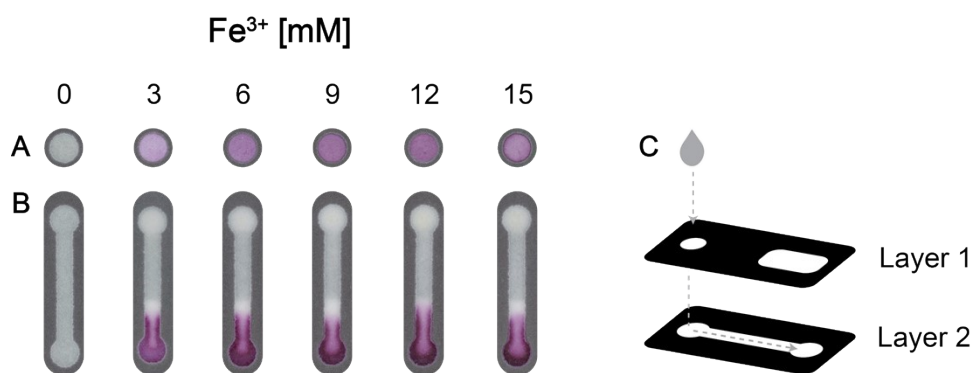


Figure S2. Modifications of channel geometry provide control over the position of the interface formed between converging fluid fronts. (A) The location of the interface (green) formed by converging fronts containing blue and yellow dyes was shifted away from the center of the detection zone (red dashed line) using an asymmetrical channel design. The detection zone is approximately 6 mm in diameter. (B) Devices assembled using the layer alignment tool and protocol described in SI. The fabrication approach consistently provides interface formation within the center zone of the detection layer for devices that contain equivalent amounts of stored dyes. Detection zones are approximately 5 mm in diameter.

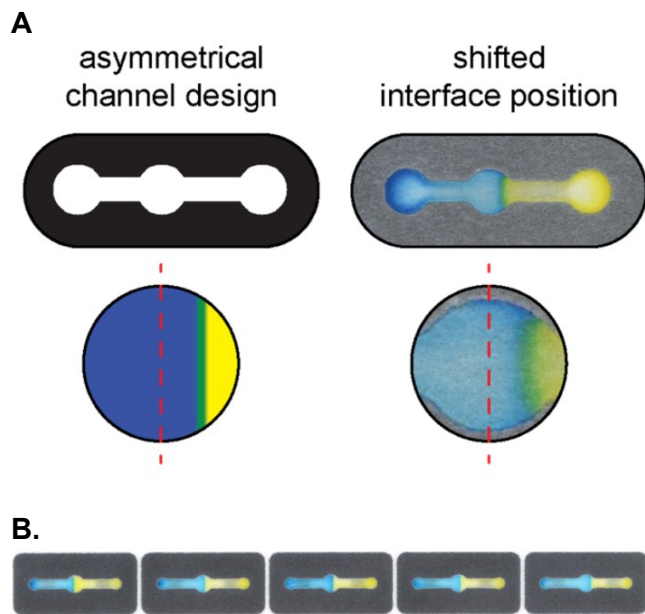


Figure S3. Multilayered paper-based devices can be assembled in strips using two opposing pins of the alignment tool. Assembling devices by this approach, which requires patterned paper and adhesive features to be geometrically aligned during additive fabrication steps, has the potential to remove user-dependent variability from our manufacturing process and reduce rates of devices failure due to layer misalignment.

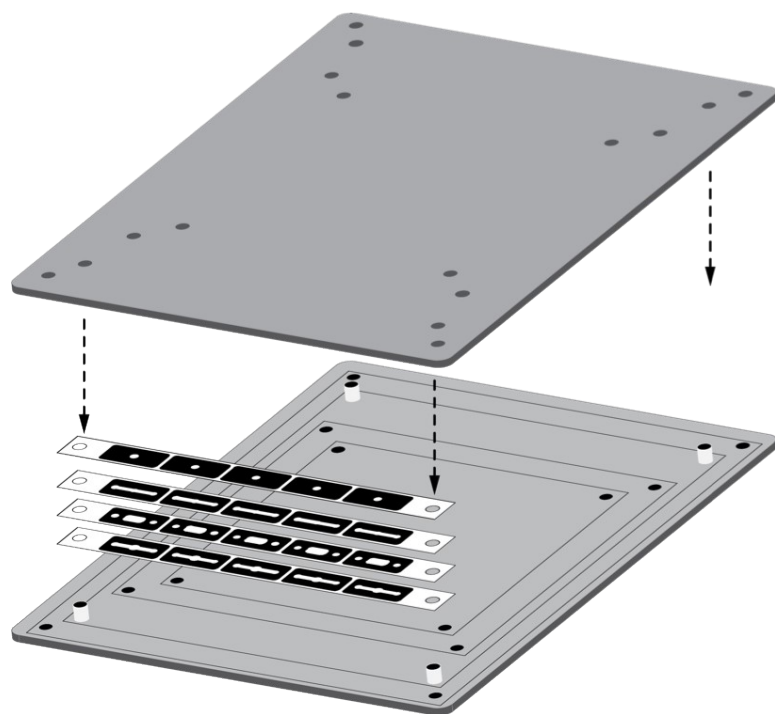


Figure S4. Schematic of the device channel layer containing the circular readout zone where assay interfaces are formed. Measurements of channel length (yellow), channel width (magenta), and zone width (blue) are provided, as is a means (red dashed line) to identify the absolute center of the readout zone that could be reached if flow from both channel inlets were perfectly timed.

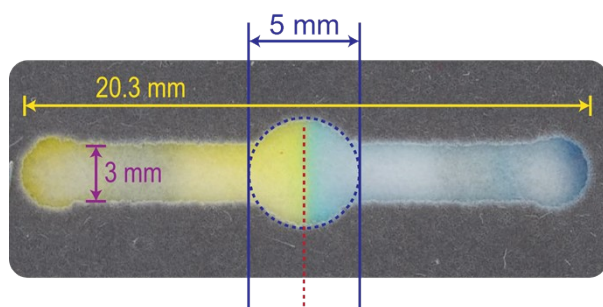


Table S1. Accuracy and precision of interface position as a function of channel width and arm length (n=10).

	Dimensions (mm)	Offset distance (mm)	CV%
Channel width	2	-0.2 ± 0.5	21
	3	-0.3 ± 0.3	13
	4	0.3 ± 0.5	17
Channel length	7	1.8 ± 0.7	17
	10	-0.3 ± 0.3	13
	13	-0.2 ± 1.1	50

Table S2. Accuracy and precision of interface position as a function of readout zone geometry (n=10).

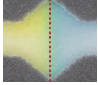
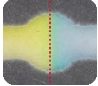
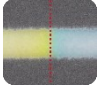
Zone shape	Image	Offset distance (mm)	CV%
Square		0.1 ± 0.4	12
Circle		-0.3 ± 0.3	13
Straight		0.0 ± 1.0	11

Figure S5. Improving signal contrast for assay interfaces using device design. The contrast of the readout zone is influenced by the pattern of the preceding layer. (A) Schematic of the three-dimensional paper-based device depicts the position of the readout zone in Layer 4 is centered below the reagent storage layer (Layer 3). (B) Grayscale intensities—where 0 is black and 255 is white, covering the full possible dynamic range of signals—demonstrate that an unpatterned section of Layer 3 backing the readout zone improves background and dynamic range. (C) Images of readout zones for devices with (i.e., fully wax-filled layer) and without (i.e., patterned feature) show visible impact of contrast control.

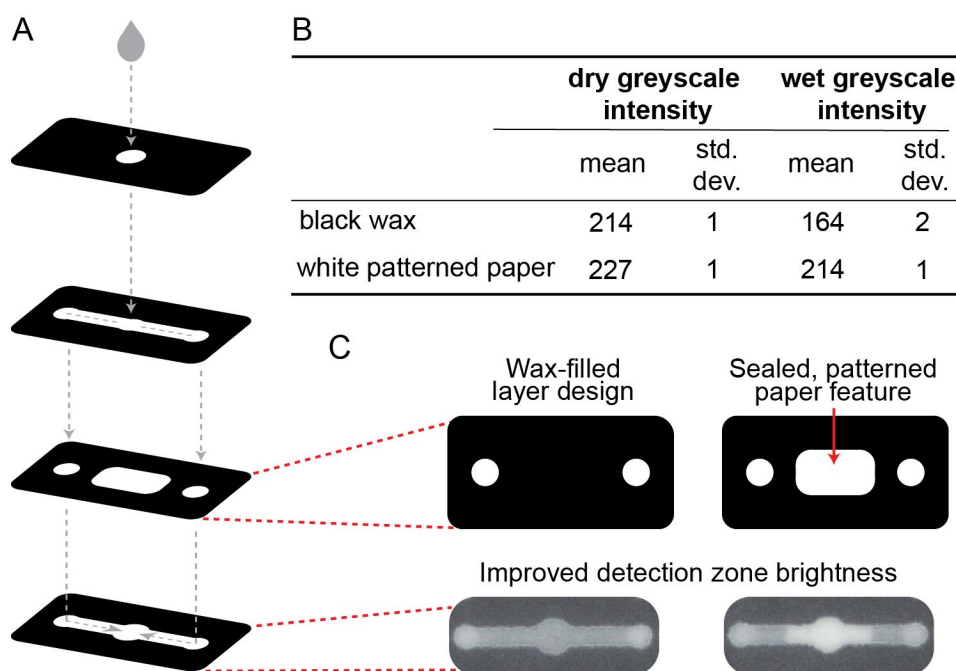


Figure S6. Full device schematic. The four wax-printed layers are backed with adhesive layers and stacked. The final wax printed layer is backed with a laminate sheet to assemble a full device.

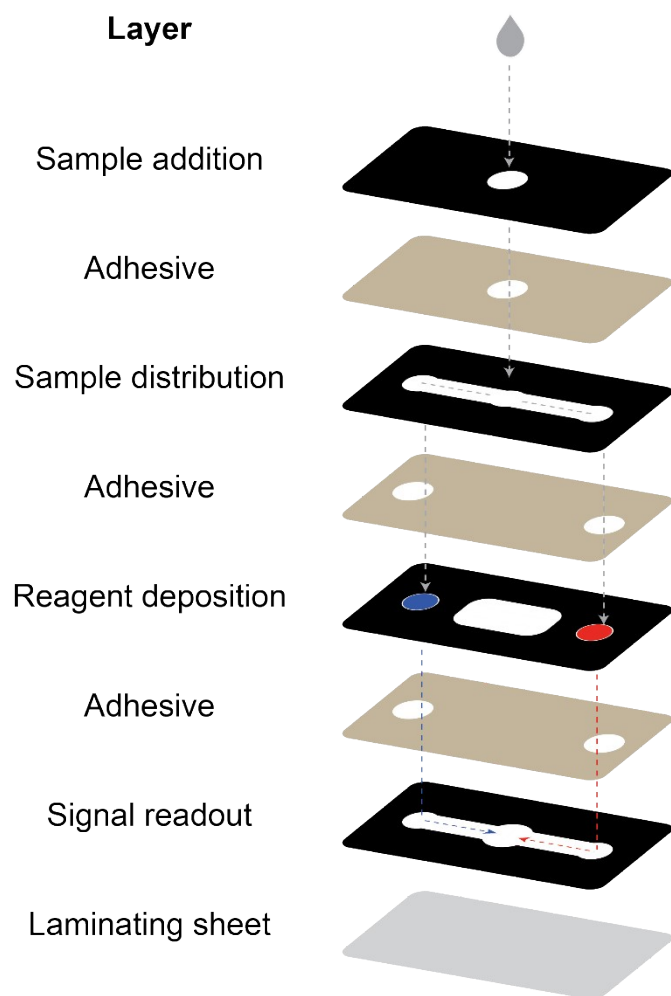


Table S3. Time needed to form interfaces as a function of paper grade using an Fe(III) assay.

Measurements of time are the mean of 5 replicates.

Paper grade	Ahlstrom				Whatman	
	54	55	601	613	1	4
Retention size (μm)	10	15	2.5	6	11	20–25
Signal formation time (min)	2–3	2	4	3–4	3	2

Table S4. Sample volume influence on signal positioning, width, and intensity (n=5).

Sample volume (μL)	Offset distance (mm)	CV%	Line width (mm)	CV%	Red channel intensity (a.u.)	CV%
20	-0.3 ± 0.5	23	0.9 ± 0.1	10	32.5 ± 7.9	24
30	-0.2 ± 0.1	3	1.1 ± 0.1	13	46.6 ± 4.1	9
40	-0.3 ± 0.3	14	0.9 ± 0.1	13	47.4 ± 6.3	13
50	-1.0 ± 0.4	29	1.0 ± 0.1	6	47.5 ± 3.6	8
75	-0.6 ± 0.4	20	0.9 ± 0.1	7	43.9 ± 5.4	12
100	0.4 ± 0.5	16	0.9 ± 0.1	8	44.0 ± 7.1	16

Figure S7. Chemical reaction scheme for the Fe(III) detection assay. Upon the addition, a sample of Fe(III) is split to distribute to opposite sides of the device and rehydrate stored reagents. In one device channel, the Fe(III) sample is reduced by ascorbic acid to produce Fe(II). In the other channel, the sample does not react with Ferrozine and solely aids in transporting the reagent to the next layer. Both liquid fronts (i.e., Fe(II) and Ferrozine) are directed toward a central detection zone where Fe(II) is chelated by Ferrozine to generate a purple product.

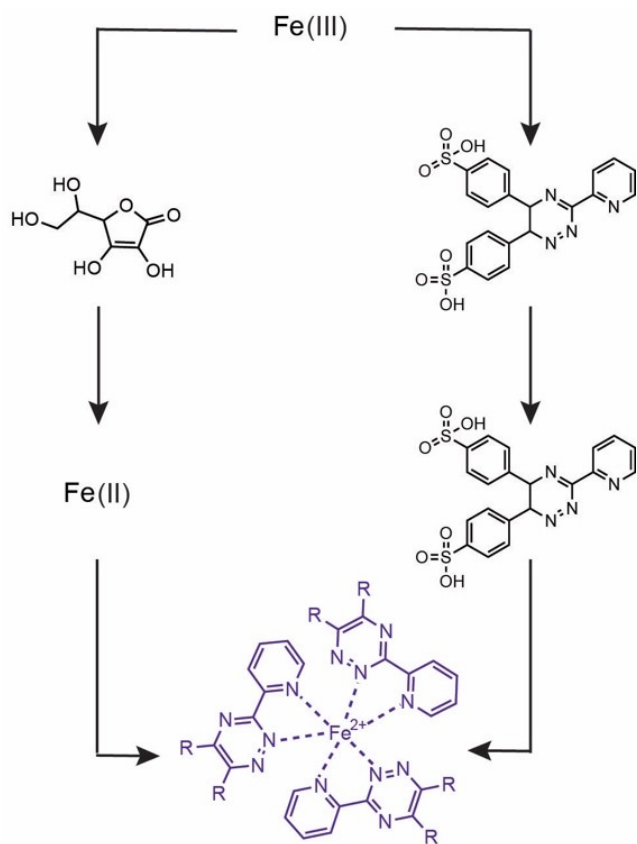


Figure S8. Detection of Fe(III) at liquid interfaces in paper-based microfluidic devices. (A) equimolar amounts of ascorbic acid and Ferrozine stored in opposite sides of the device enabled detection of millimolar concentrations of Fe(III), but the advancing front of the channel containing Ferrozine contributed a substantial amount of background signal. To diminish the presence of this undesired color that could mask the formation of positive signals, we treated the reagent distribution channel with EDTA. (B) EDTA-treated devices were used to measure sample concentrations corresponding to the amounts of Fe(III) that could be liberated from solutions containing physiologically relevant quantities of hemoglobin (12–18 g/dL). These signals could then be distinguished by visual inspection or measured by image analysis.

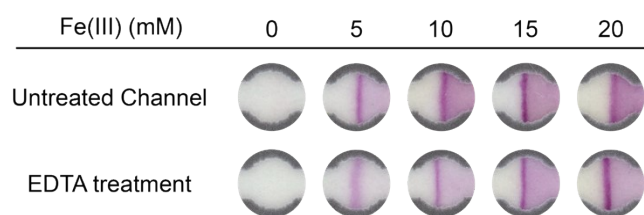


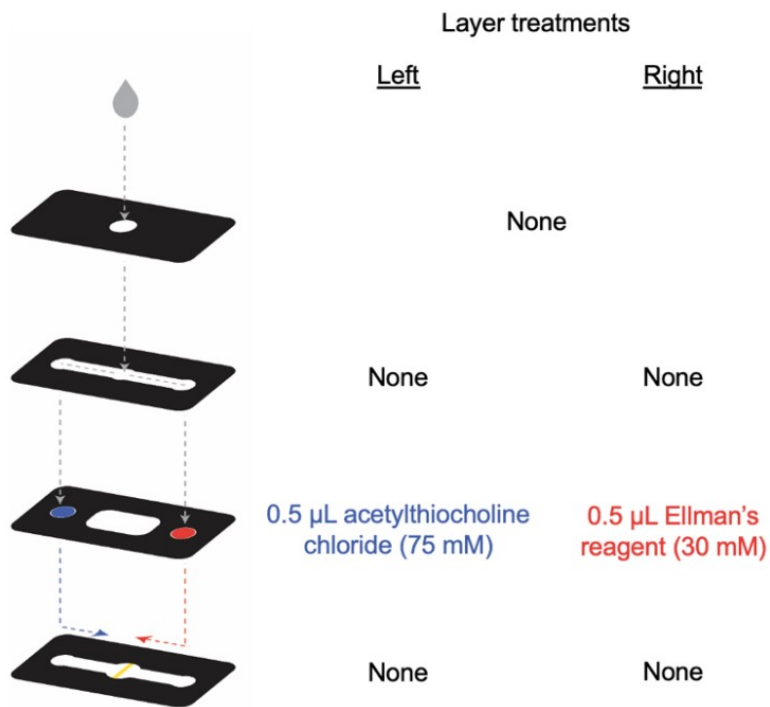
Table S5. Signal-to-background ratio (S:B) resulting from using different concentrations of Ferrozine in Fe(III) assay in the presence and absence of 100 mM EDTA. Measurements are the mean of 5 replicates.

S:B	[Ferozine] (mM)			
	10	25	50	100
without EDTA	0.80	1.12	1.59	1.64
with EDTA	1.12	1.45	1.61	1.87

Table S6. Signal-to-background ratio (S:B) for assays for 100 mM Fe(III) using different concentrations of EDTA. Measurements are the mean of 5 replicates.

[EDTA] (mM)	0	10	25	50	75	100	200	300	400	500
S:B	1.32	1.41	1.44	1.53	1.57	1.81	2.00	1.71	1.70	1.77

Figure S9. Device layer treatments for the AChE assay. The reagent storage layer (device layer 3) is the only layer treated with reagents for this assay. One zone is treated with 0.5 μ L acetylthiocholine chloride (75 mM) and the other zone is treated with 0.5 μ L of Ellman's reagent (30 mM). The dotted line indicates fluid flow throughout the device where sample addition allows fluid to distribute to opposite sides of the device and rehydrate stored reagents. After rehydration, solutions are directed toward a central detection zone where they meet to form a yellow liquid interface. The detection zone is approximately 5 mm in diameter.



interface. The detection zone is approximately 5 mm in diameter.

Figure S10. Device layer treatments for the lactate assay. The sample addition layer (device layer 1) is not treated with any reagents. On the sample distribution layer (device layer 2), the left side of the device is treated with 2 μL NAD^+ (30 mM) and lactate dehydrogenase (LDH, 1 mg/mL) and the right side of the device is treated with 2 μL 3-(4,5-dimethylthiazol-2-yl)-2,5-diphenyltetrazolium bromide (MTT, 10 mM). On the reagent storage layer (device layer 3), the left side of the device is treated with 1.5 μL NAD^+ (30 mM) and Lactate dehydrogenase (LDH, 1 mg/mL), and the right side of the device is treated with 1.5 μL phenazine methosulfate (PMS, 10 mM). Finally, on the interface formation layer (device layer 4), the left side of the device is treated with 2.5 μL of hydrazine buffer (pH 9.7) and the right side of the device is left untreated. The dotted line indicates fluid flow throughout the device where sample addition allows fluid to distribute to opposite sides of the device and rehydrate stored reagents. After rehydration, solutions are directed toward a central detection zone where they meet to form a purple liquid interface. The detection zone is approximately 5 mm in diameter.

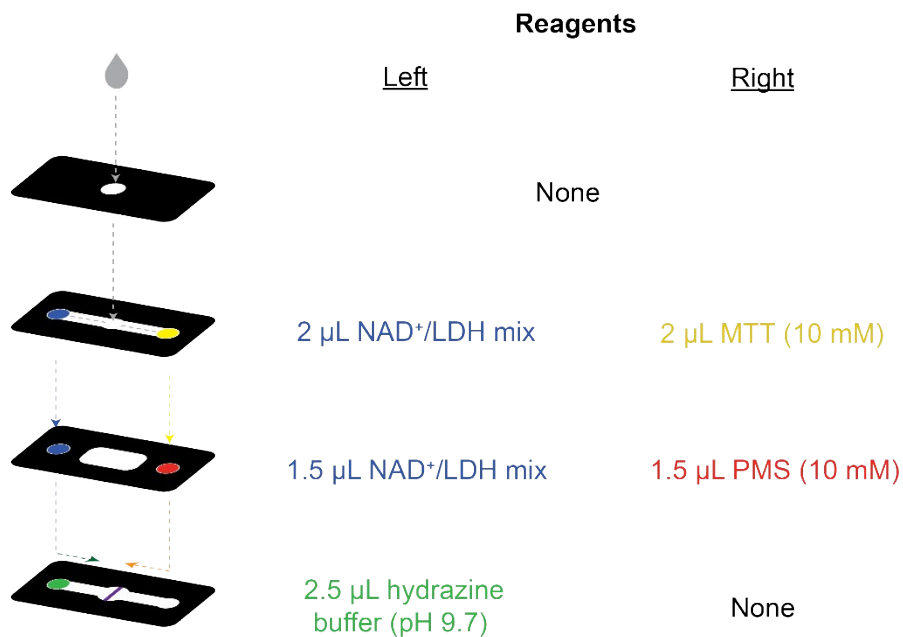


Figure S11. Device layer treatments for the formation of assays outputs at multiple interface (Fe(III), AChE, and their respective controls). The sample addition layer (device layer 1) is not treated with any reagents. On the sample distribution layer (device layer 2), zones 1 to 3 are not treated with any reagents and zone 4 is treated with 2 μL of EDTA (100 mM). On the reagent storage layer (device layer 3), zone 1 is treated with 0.5 μL cysteine, 5,5'-dithiobis(2-nitrobenzoic acid) (DTNB, Ellman's reagent, 30 mM), zone 2 is treated with 0.5 μL $\text{FeCl}_2 \cdot 4\text{H}_2\text{O}$ (5 mM) and 0.5 μL cysteine (0.5 M), zone 3 is treated with 0.5 μL ascorbic acid (AA, 100 mM) and 0.5 μL acetylthiocholine (ATC, 75 mM), and zone 4 is treated with 0.5 μL of Ferrozine (100 mM). Finally, the interface formation layer (device layer 4) is not treated with any reagents. The dotted line indicates fluid flow throughout the device where sample addition allows fluid to distribute to opposite sides of the device and rehydrate stored reagents. After rehydration, solutions are directed toward a central detection zone. The detection zone is approximately 5 mm in diameter.

